Supporting information

Extending the π-Conjugation System of Covalent Organic Frameworks for more Efficient Photocatalytic H_2O_2 Production

Maojun Deng[a], Jiamin Sun[a], Andreas Laemont[a], Chunhui Liu[a], Linyang Wang[a], Laurens Bourda[a,b], Jeet Chakraborty[a] , Kristof Van Hecke[b], Rino Morent[c], Nathalie De Geyter[c], Karen Leus[a,c], Hui Chen[a*] and Pascal Van Der Voort[a*]

[a] COMOC-Center for Ordered Materials, Organometallics and Catalysis, Department of Chemistry, Ghent University, Krijgslaan 281-S3, 9000 Ghent, Belgium.
[b] XStruct, Department of Chemistry, Ghent University, Krijgslaan 281-S3, 9000 Ghent, Belgium
[c] RUPT-Research Unit Plasma Technology, Department of Applied Physics, Ghent University, Sint-Pietersnieuwstraat 41 B4, 9000 Gent, Belgium.

* Corresponding Authors: huichen@xauat.edu.cn, Pascal.Vandervoort@ugent.be

Experimental Section

1. Materials and Instrumentation

Materials All the chemicals were purchased from Sigma-Aldrich, Fluorochem or TCI Europe and used without further purification.

Instrumentation

Diffuse Reflectance Infrared Fourier Transform Spectroscopy (DRIFTS) measurements were recorded on a Nicolet 6700 spectrometer (Thermo Scientific) in a KBr matrix. Thermogravimetric analysis (TGA) was performed on a Netzsch STA 449 F3 Jupiter within a temperature range of 20-800 °C in N_2 with a heating rate of 10 °C/min. Powder X-ray diffraction (PXRD) patterns were collected on a Bruker D8 Advance diffractometer equipped with an autochanger and LynxEye XE-T Silicon strip Line detector, operated at 40 kV, 30 mA using Cu-Kα radiation (λ = 1.5406 Å) in Bragg-Brentano geometry. Nitrogen

adsorption experiments were performed at 77 K using a 3P instrument micropore analyzer. The samples were activated before the measurements by heating at 120 °C for 12 hours under vacuum. For ^{1}H NMR analysis, the samples were dissolved in DMSO-*d6*. The spectra were recorded on a Bruker 400 MHz AVANCE spectrometer. Elemental analyses (C, N, H, S) were carried out on a Thermo Scientific Flash 2000 CHNS-O analyzer equipped with a TCD detector. The surface chemical composition of the samples was investigated by X-ray photoelectron spectroscopy (XPS) using the PHI 5000 VersaProbe II spectrometer equipped with a monochromatic Al Kα X-ray source (hν = 1486.6 eV). To do so, the samples were excited with an X-ray beam (size: 200 μm) over an area of 500 x 500 μm^2 at a power of 50 W. Wide range survey scans and high-resolution spectra were recorded with a pass energy of 187.85 eV and 23.5 eV and a step size of 0.8 eV and 0.1 eV respectively. All spectra were acquired at a take-off angle of 45° relative to the sample surface in the XPS chamber where the pressure was constantly maintained below 10^{-6} Pa. Zeta potentials of the samples at different pHs were determined by the Zetasizer (NanoZS) from Malvern Instruments.

Synthesis of organic linkers and COFs

1.1 Synthesis of 4,4',4'',4'''-(ethene-1,1,2,2-tetrayl)tetraaniline (4PE)

4,4',4'',4'''-(ethene-1,1,2,2-tetrayl)tetraaniline (4PE) is synthesized following the published procedure.[1] The specific synthesis route of 4PE is shown below. (**Scheme S1**) ^{1}H NMR (400 MHz, DMSO-d_6) δ (ppm): 6.60-6.55 (m, 8H), 6.29-6.24 (m, 8H), 4.84 (s, 8H). (**Figure. S1**)

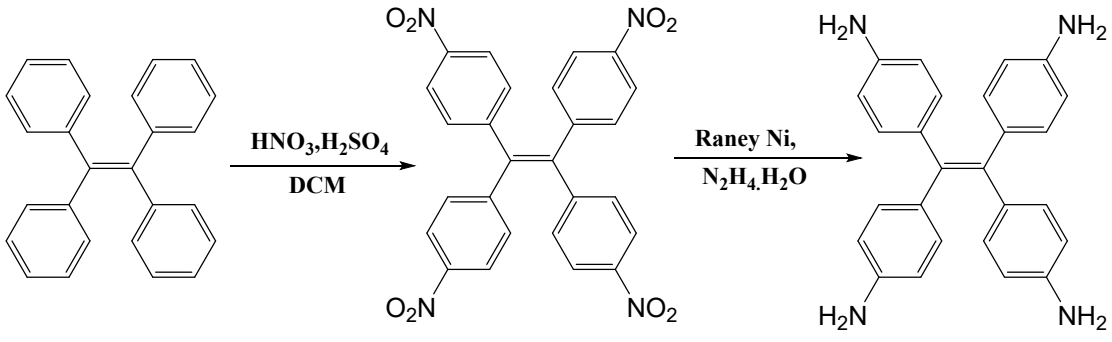

Scheme S1. The synthesis of4,4',4'',4'''-(ethene-1,1,2,2-tetrayl)tetraaniline (4PE).

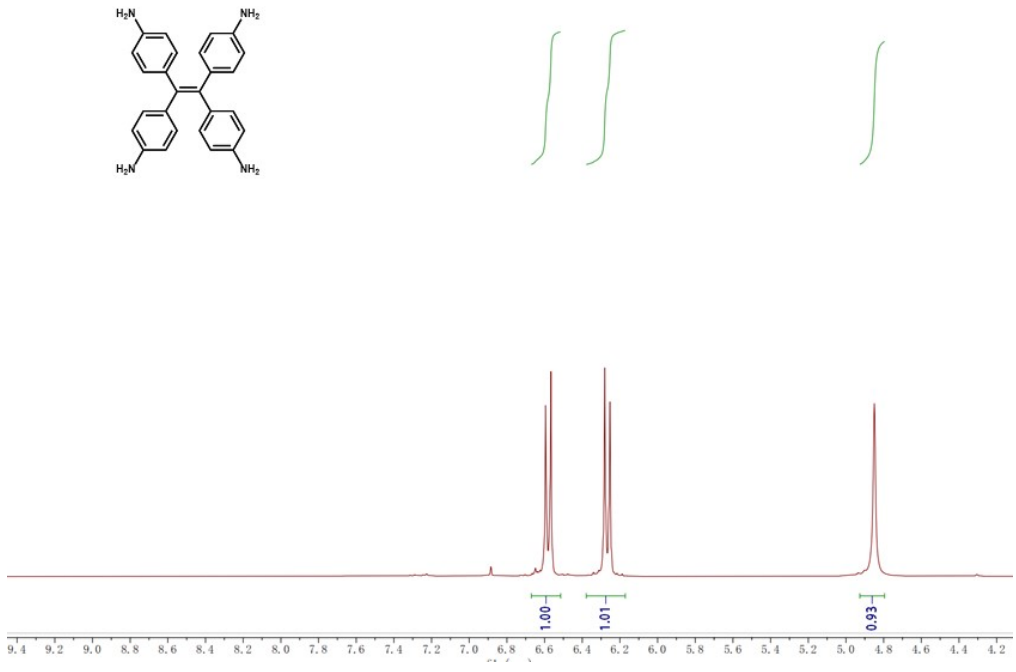

Figure S1. ^{1}H NMR spectrum of 4,4',4",4"'-(ethene-1,1,2,2-tetrayl)tetraaniline (4PE)

1.2 Synthesis of Naphthalene-2,6-dicarbaldehyde (N)

Naphthalene-2,6-dicarbaldehyde (N) is synthesized following the published procedure.[2] The specific synthesis route of N is shown below. (**Scheme S2**) ^{1}H NMR (400 MHz, DMSO-d_6) δ (ppm):10.22 (s, 2H), 8.70 (m, arom), 8.32 (dd, J= 8.4, 1.7 Hz, 2H, arom), 8.05 (dd, J= 8.4, 1.7 Hz, 2H, arom). (**Figure. S2)**

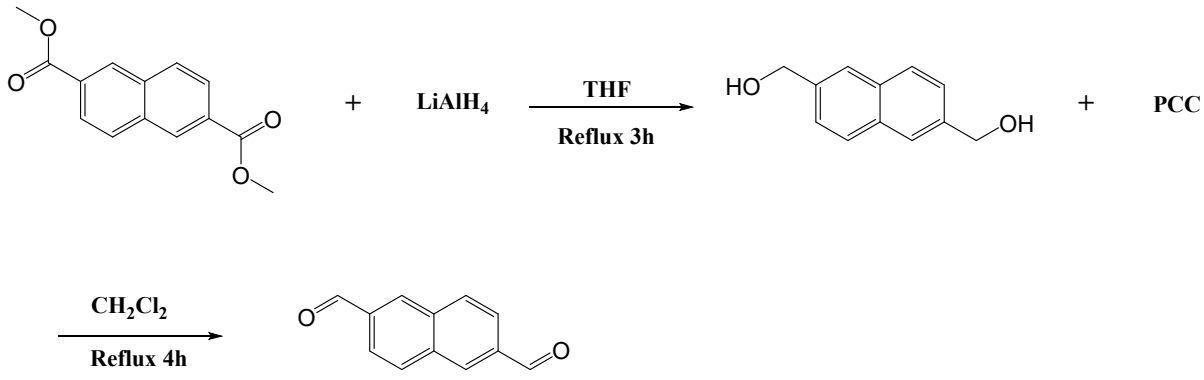

Scheme S2. The synthesis of Naphthalene-2,6-dicarbaldehyde (N)

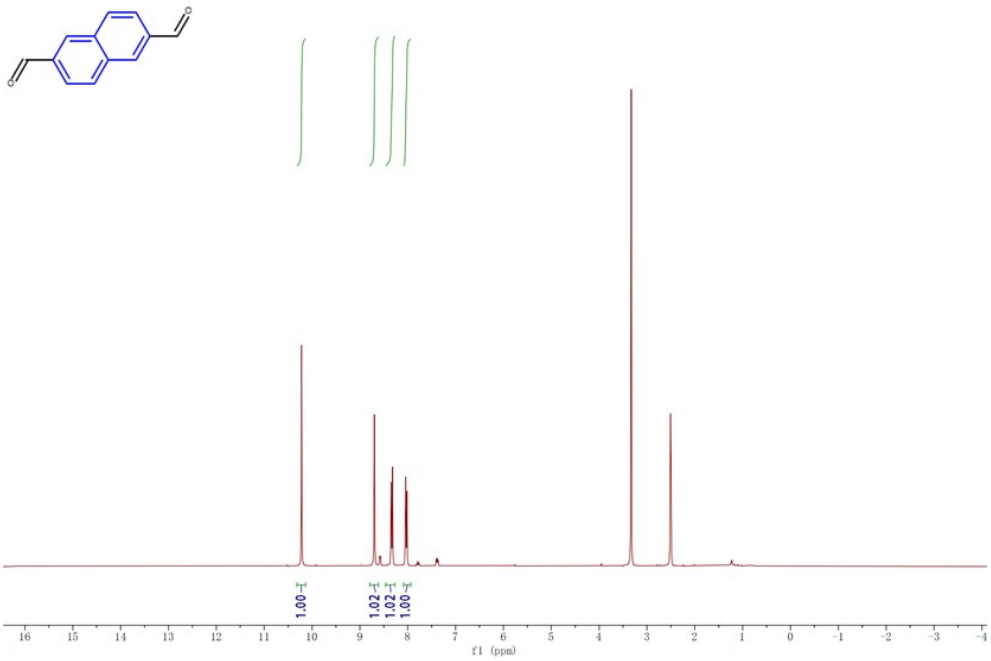

Figure S2. ^{1}H NMR spectrum of naphthalene-2,6-dicarbaldehyde (N)

1.3 Synthesis of 4PE-N-COF

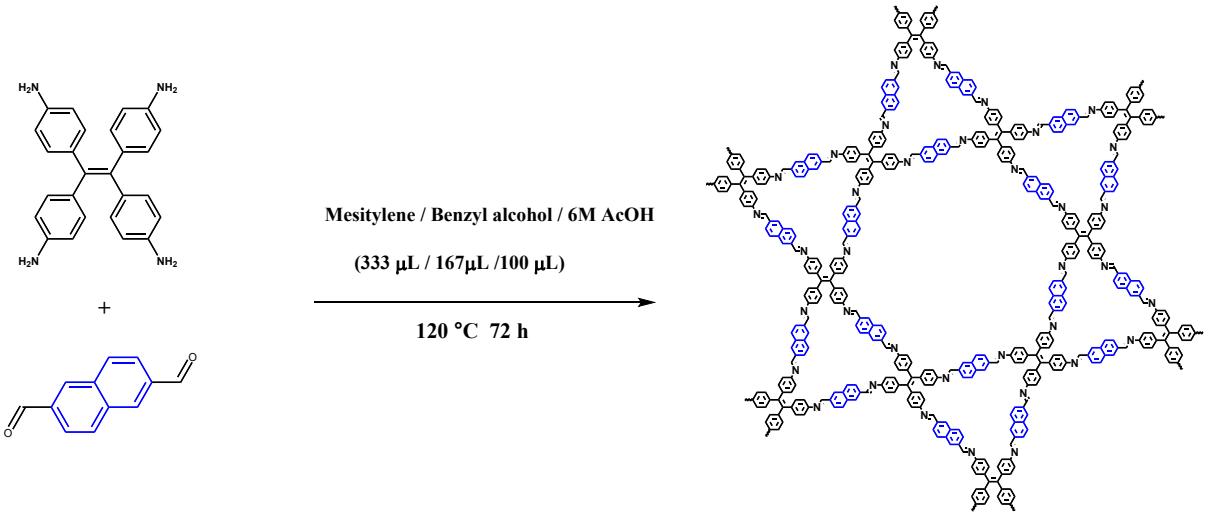

In a 10 mL Pyrex tube, 4,4',4",4"'-(ethene-1,1,2,2-tetrayl)tetraaniline (4PE, 7.85 mg, 20 μmol) and Naphthalene-2,6-dicarbaldehyde (N, 7.4 mg, 40 μmol) was added in an ampoule. Then 333 µL mesitylene and 167 µL benzyl alcohol were added to the ampoule. Finally, 100 µL 6M acetic acid (AcOH) was added. The mixture was sonicated for 15 minutes and then degassed via a freeze-pump-

thaw procedure for 3 cycles. The ampoule was flame-sealed and heated at 120 °C for 72 hours. The precipitate was collected through filtration, washed with acetone (3 × 20 mL) and tetrahydrofuran (THF) (3 × 20 mL) to remove unreacted monomers. Afterwards, the yellow solid was washed using Soxhlet extraction with THF for 6 hours. The powder was collected and dried at 120 °C under vacuum overnight to produce 4PE-N COF as a yellow solid in 85% isolated yield.

1.4 Synthesis of 4PE-N-S COF

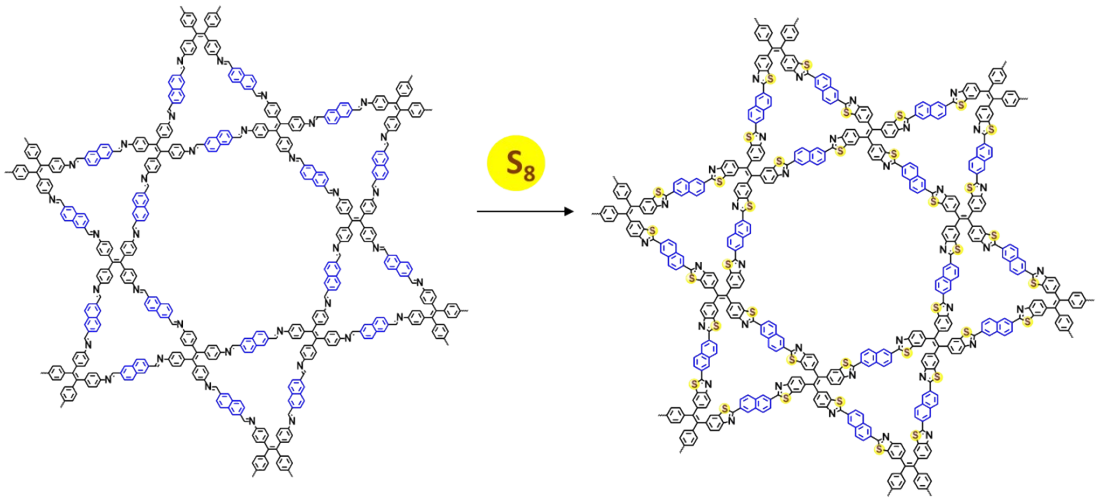

The 4PE-N-COF (20 mg) was activated under high vacuum at 120 °C and subsequently mixed with sulfur (200 mg) in a 10 ml glass vial. The mixtures where then stirred with a magnetic stirring bar for 10 minutes (1200 rpm) until a visually homogeneous mixture is formed. The resulting mixture was transferred into an ampoule and flame sealed under vacuum. Then the ampoule was heated at 150°C (5°C min^{-1} heating rate) for 3 hours and then raised to 300 °C (1.67°C min^{-1} heating rate) and kept for 2.5 hours at this temperature. After cooling down, the resulting brown powder was soaked in a mixture solvent of chlorobenzene and 1,2-dichlorobenzene (V/V=4:6) at 80 °C. The powder was collected and dried at 120 °C under vacuum overnight.

2.5 Synthesis of 4PE-TT COF

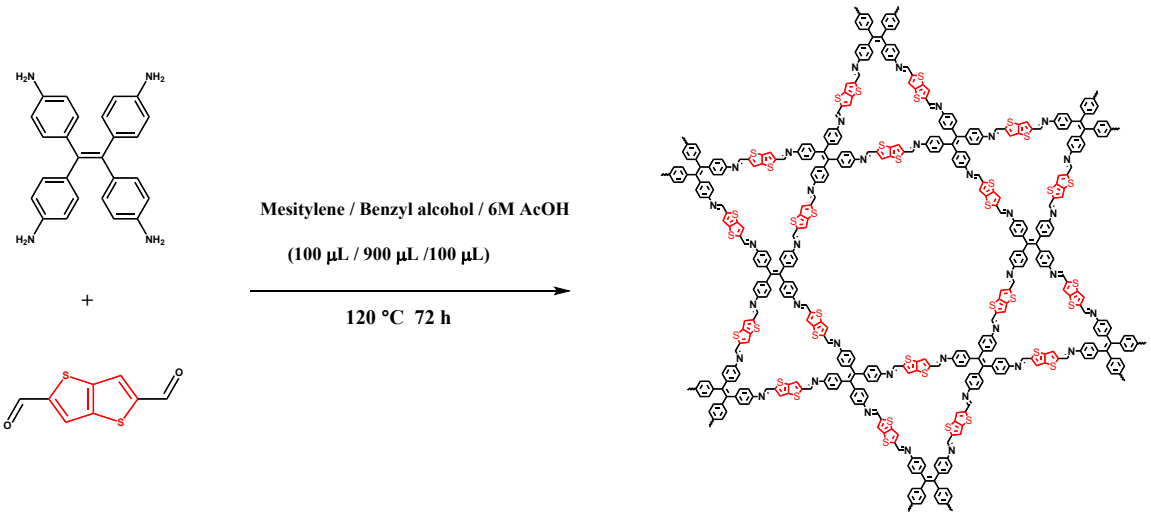

The 4PE-TT COF was synthesized according to a previously described method.[3] In a 10 mL Pyrex tube, 4,4',4",4"'-(ethene-1,1,2,2-tetrayl)tetraaniline (4PE, 23.6 mg, 60 μmol) and thieno[3,2-b]thiophene-2,5-dicarboxaldehyde (TT, 23.6 mg, 120 μmol) were added in an ampoule. Then 100 µL mesitylene and 900 µL benzyl alcohol were added to the ampoule. Finally, 100 µL 6M acetic acid (AcOH) was added. The mixture was sonicated for 15 minutes and then degassed via a freeze-pump-thaw procedure for 3 cycles. The ampoule was flame-sealed and heated at 120 °C for 72 hours. The precipitate was collected through filtration, washed with acetone (3 × 20 mL) and tetrahydrofuran (THF) (3 × 20 mL) to remove unreacted monomers. Afterwards, the red solid was washed using a Soxhlet extraction with THF for 6 hours. The powder was collected and dried at 120 °C under vacuum overnight to produce 4PE-N COF as a yellow solid in 82% isolated yield.

2. Structure simulations and powder X-ray diffraction (PXRD) analyses:

Table S1: Unit cell parameters and atom positions of the 4PE-N COF crystal structure fitted by Material Studio.

Atom List	x	y	z

C1	1.00128	0.48394	-0.04252
C2	0.96592	0.44913	-0.09220
C3	0.96824	0.51963	-0.08650
C4	0.95784	0.53757	0.08728
C5	0.92596	0.53893	0.04950
C6	0.90367	0.52157	-0.15886
C7	0.91475	0.50464	-0.33772
C8	0.94730	0.50457	-0.30419
C9	0.93696	0.43744	0.07815
C10	0.90429	0.40533	0.03490
C11	0.90047	0.38356	-0.17392
C12	0.92941	0.39509	-0.34565
C13	0.96174	0.42784	-0.30614
N14	0.86670	0.35038	-0.20774
N15	0.87052	0.52240	-0.18767
C16	0.84106	0.49628	-0.28707
C17	0.68063	0.54189	-0.31423
H18	0.97441	0.55058	0.25148
H19	0.91812	0.55271	0.18617
H20	0.89870	0.49215	-0.50514
H21	0.95622	0.49259	-0.446
H22	0.93944	0.45339	0.24271

H23	0.88212	0.39693	0.16779
H24	0.92688	0.37921	-0.51207
H25	0.98352	0.43648	-0.44191
H26	0.83966	0.47101	-0.34121
H27	0.68188	0.56688	-0.37426
C28	0.17699	-0.25408	-0.34339
C29	0.17470	-0.28811	-0.32785
C30	0.20677	-0.29002	-0.31865
C31	0.24081	-0.25815	-0.31981
C32	0.24283	-0.22390	-0.32525
C33	0.21078	-0.22218	-0.33969
C34	0.27288	-0.25990	-0.31380
C35	0.30666	-0.22802	-0.30889
C36	0.30888	-0.19397	-0.30454
C37	0.27684	-0.19201	-0.31471
H38	0.15254	-0.25216	-0.35165
H39	0.20523	-0.31625	-0.31042
H40	0.21183	-0.19618	-0.34637
H41	0.27184	-0.28590	-0.31177
H42	0.33111	-0.22995	-0.30256
H43	0.27841	-0.16576	-0.31557

Table S2: Unit cell parameters and atom positions of the 4PE-N-S COF crystal structure fitted by Material

Studio.

Atom List	x	y	z
C1	0.99681	0.48126	-0.14051
C2	0.95865	0.44801	-0.13042
C3	0.97216	0.52729	-0.14009
C4	0.97395	0.55550	0.02958
C5	0.94493	0.56352	0.03547
C6	0.91409	0.54297	-0.12768
C7	0.91202	0.51568	-0.29319
C8	0.94087	0.50792	-0.30602
C9	0.93197	0.44617	0.05265
C10	0.89631	0.41510	0.06433
C11	0.88792	0.38527	-0.10396
C12	0.91381	0.38583	-0.27769
C13	0.94928	0.41698	-0.29634
N14	0.85526	0.35374	-0.10815
N15	0.88365	0.54621	-0.12975
C16	0.85814	0.52067	-0.29739
C17	0.67020	0.52666	-0.28494
H18	0.99755	0.57095	0.15978
H19	0.94617	0.58465	0.16877
S20	0.87094	0.49214	-0.45911

H21	0.93801	0.48577	-0.43055
H22	0.93868	0.46937	0.17952
H23	0.87591	0.41425	0.20338
S24	0.89796	0.34552	-0.45295
H25	0.96921	0.41699	-0.43537
C28	0.17099	-0.26135	-0.34697
C29	0.17576	-0.29232	-0.32126
C30	0.21176	-0.28720	-0.31346
C31	0.24281	-0.25141	-0.32546
C32	0.23784	-0.22020	-0.33838
C33	0.20182	-0.22549	-0.35296
C34	0.27876	-0.24629	-0.31985
C35	0.30957	-0.21053	-0.32039
C36	0.30490	-0.17935	-0.32140
C37	0.26896	-0.18430	-0.33212
H38	0.14342	-0.26478	-0.35194
H39	0.21553	-0.31110	-0.29621
H40	0.19748	-0.20192	-0.36520
H41	0.28305	-0.26992	-0.31174
H42	0.33707	-0.20725	-0.31031
H43	0.26531	-0.16025	-0.33509

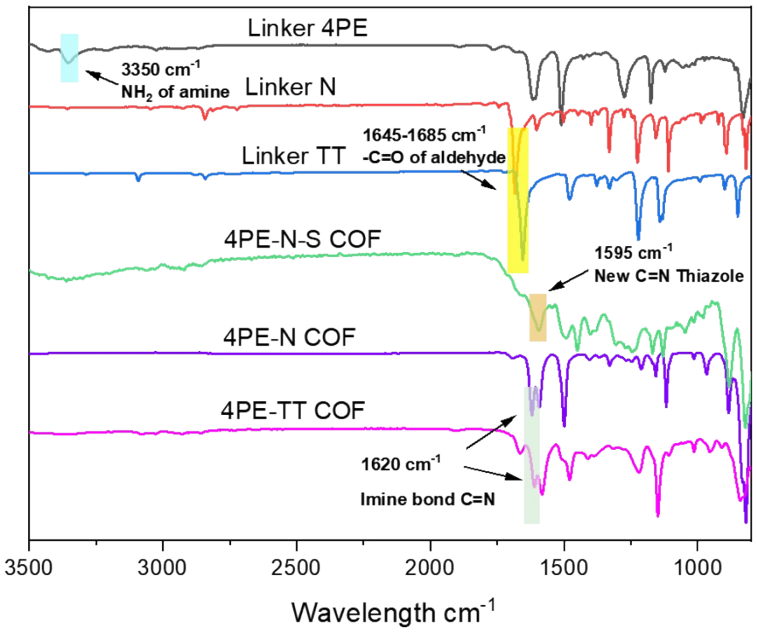

Figure S3. FT-IR spectrum of the organic linkers (4PE, N, TT), 4PE-N, 4PE-N-S and 4PE-TT COF.

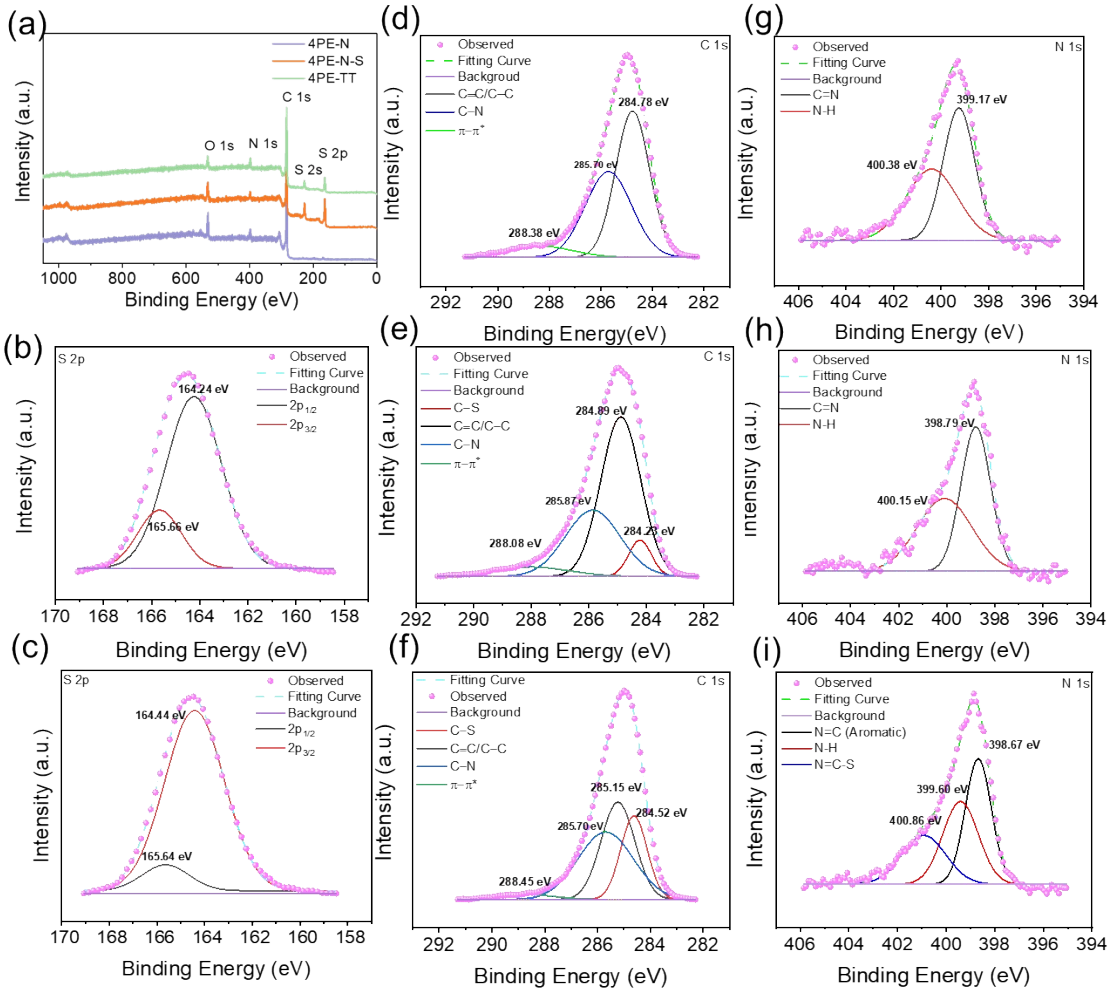

Figure S4. (a) Survey XPS spectrum of all samples. XPS high resolution spectra of 4PE-TT (b) and 4PE-

N-S (c) in the region of S 2p. XPS high resolution spectra of 4PE-N (d), 4PE-TT (e) and 4PE-N-S (f) in the region of C 1s. XPS high resolution spectra of 4PE-N (g), 4PE-TT (h) and 4PE-N-S (i) in the region of N 1s.

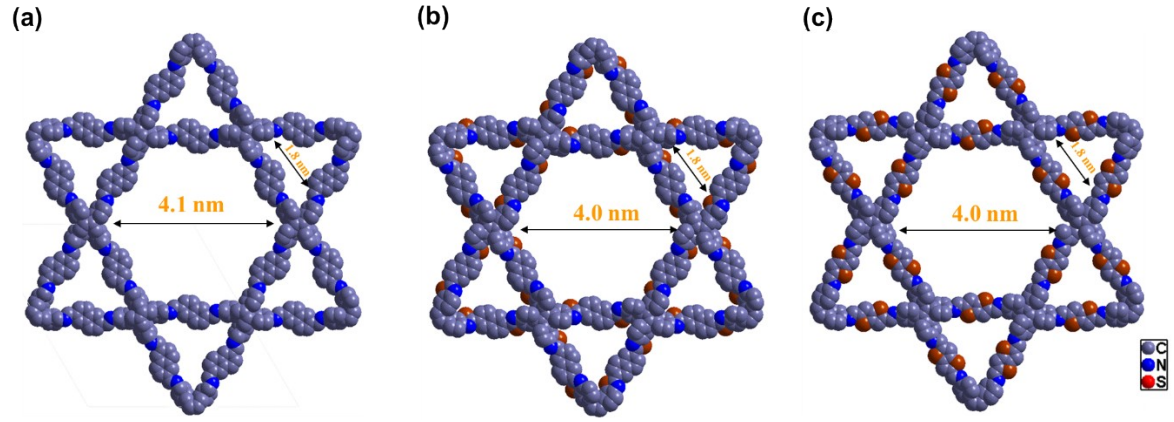

Figure S5. Images of the crystal structures of the dual-pore Kagome (a) 4PE-N, (b) 4PE-N-S and (C) 4PE-TT COF in AA stacking modes.

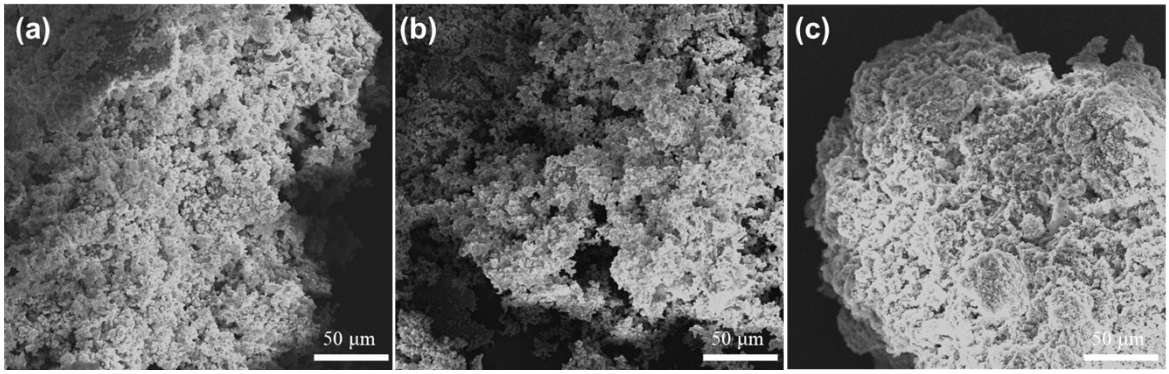

Figure S6. SEM image of 4PE-N (a), 4PE-N-S (b) and 4PE-TT (c).

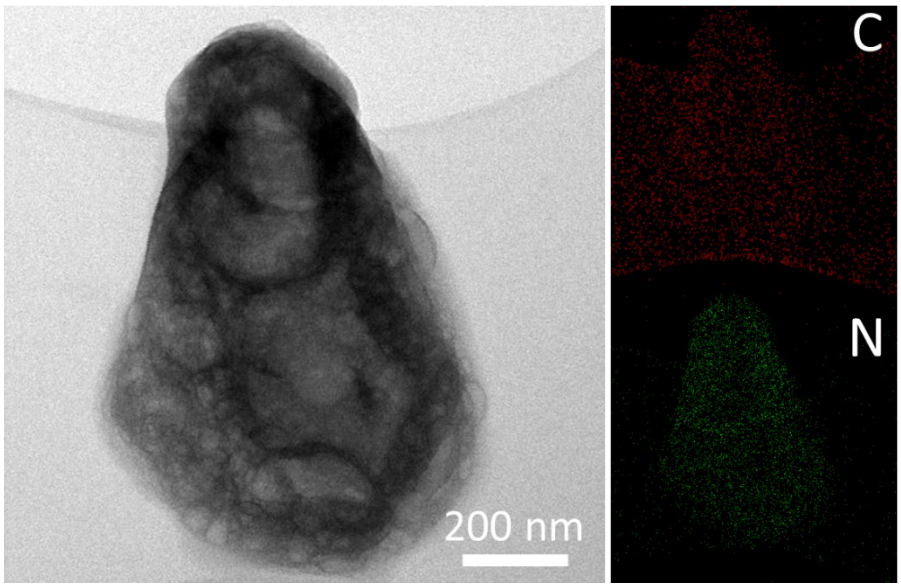

Figure S7. TEM images and the corresponding elemental mapping of C (red) and N (green) for 4PE-N COF.

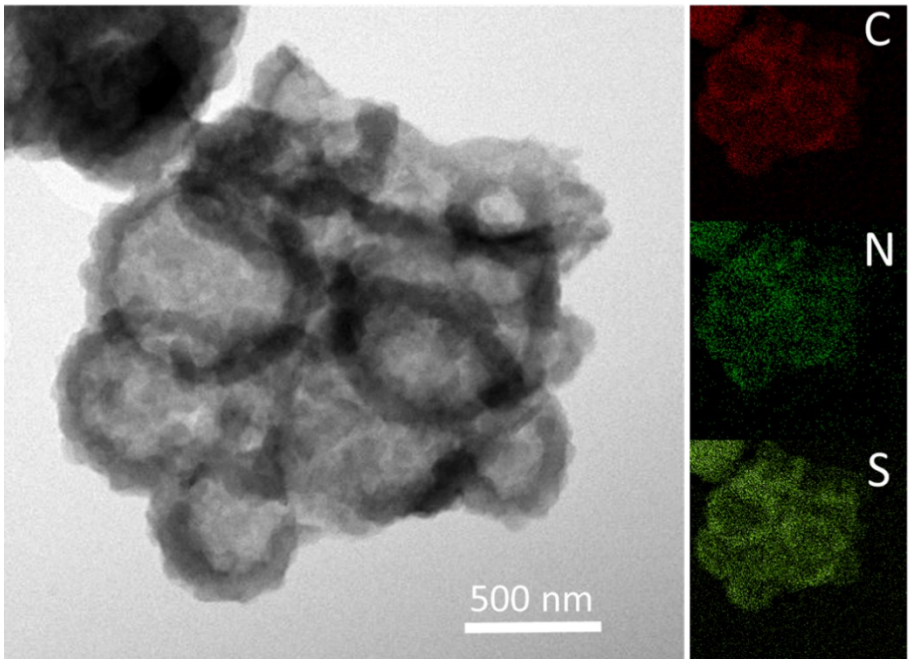

Figure S8. TEM images and the corresponding elemental mapping of C (red), N (green) and S (yellow) for 4PE-N-S COF.

4. Characterization data.

Table S3. Elemental analysis of COFs.

COF[a]	C (wt%)		H (wt%)		N (wt%)		S (wt%)	
	Calc.	Exp.	Calc.	Exp.	Calc.	Exp.	Calc.	Exp.
4PE-N（$C_{50}H_{32}N_4$）	87.18,	86.80	4.69,	4.30	8.14,	7.87	–,	–
4PE-N-S（$C_{50}H_{28}N_4S_4$）	73.86,	73.74	3.48,	3.52	6.89,	6.51	15.77,	15.07
4PE-TT（$C_{42}H_{24}N_4S_4$）	70.75,	69.87	3.39,	3.06	7.86,	6.74	17.99,	16.68

[a]: Calc. = calculated data; Exp. = experimental results.

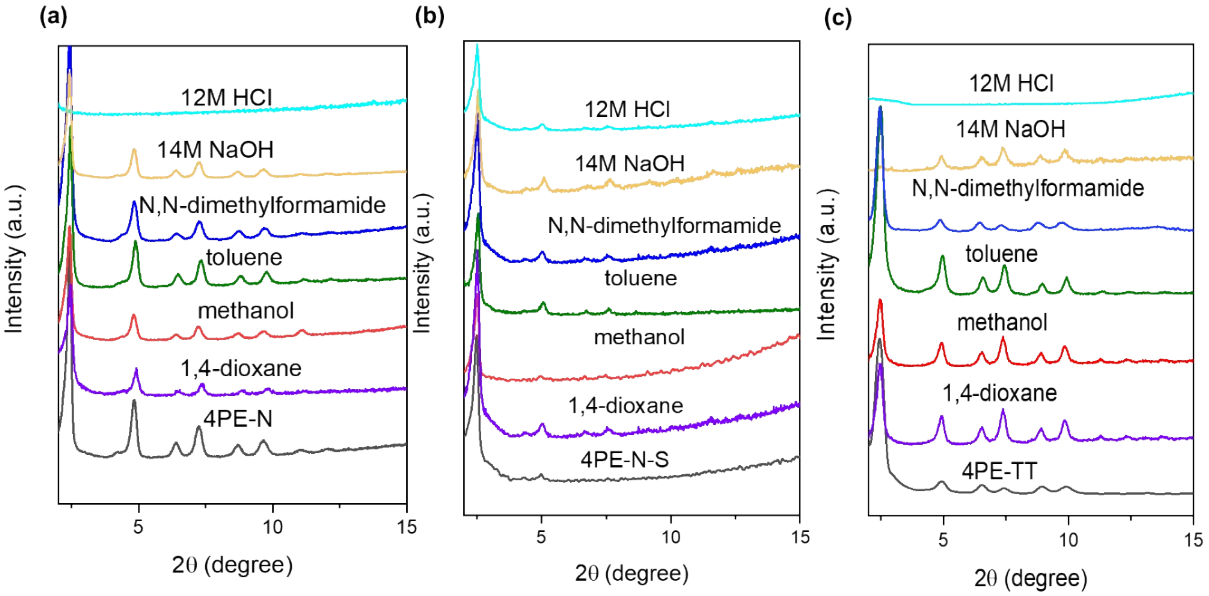

Figure S9. The pristine PXRD patterns of the (a) 4PE-N, (b) 4PE-N-S and (c) 4PE-TT COF after treatment in different media.

Table S4: The crystallinity of studied COFs in different media. [a]

COF	Different Media	Crystallinity
4PE-N COF	Pristine COF	81%
	12M HCl	<5%
	14M NaOH	34%
	Methanol	74%
	DMF	38%

	Toluene	40%
	1,4-dioxane	50%
4PE-N-S COF	Pristine COF	56%
	12M HCl	44%
	14M NaOH	53%
	Methanol	54%
	DMF	41%
	Toluene	46%
	1,4-dioxane	43%
4PE-TT	Pristine COF	70%
	12M HCl	<5%
	14M NaOH	32%
	Methanol	65%
	DMF	52%
	Toluene	64%
	1,4-dioxane	63%

[a]: obtained from Diffrac. Eva by calculating the ratio of area under sharp peaks versus total area under the curve (2θ: range 2-40º).

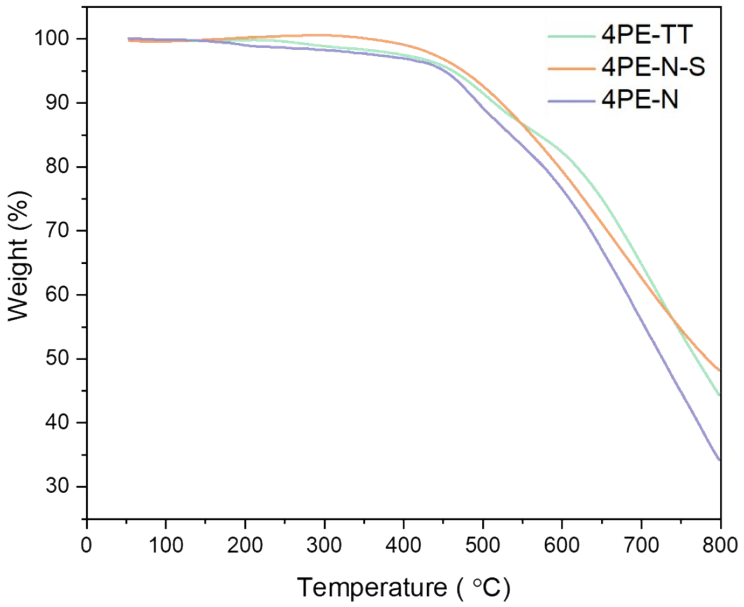

Figure S10. TGA of 4PE-N, 4PE-N-S and 4PE-TT COF.

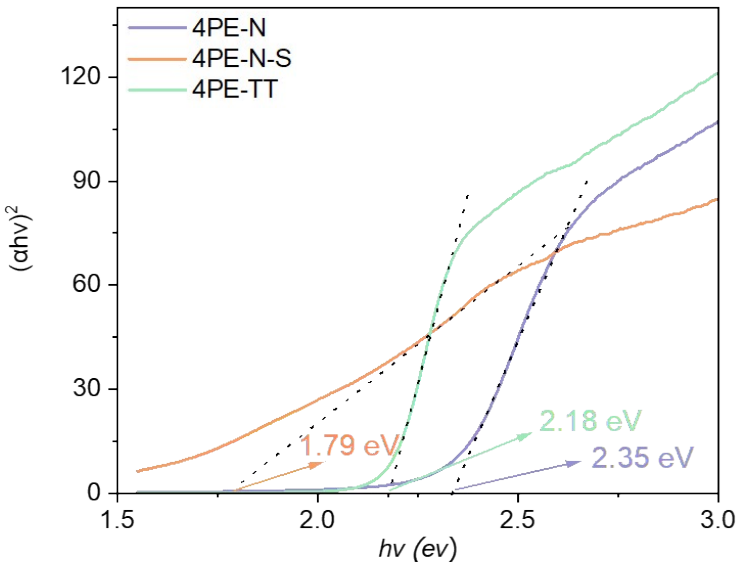

Figure S11. Tauc plots of 4PE-N, 4PE-N-S and 4PE-TT COF.

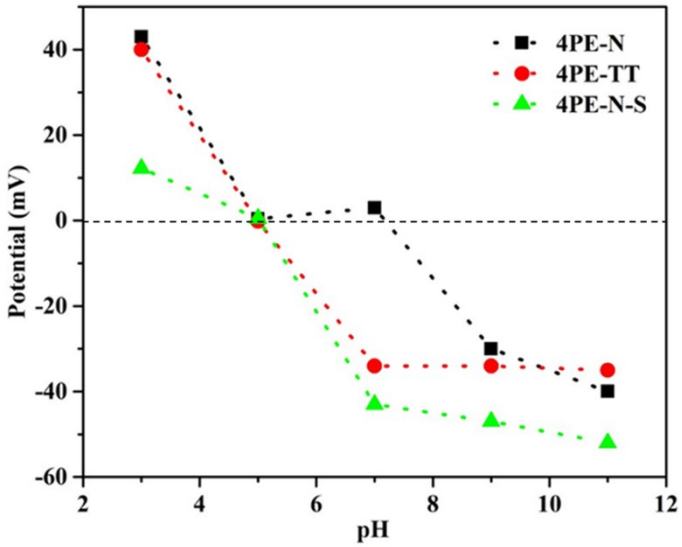

Figure S12. The Isoelectric point measurement for 4PE-N, 4PE-N-S and 4PE-TT COF.

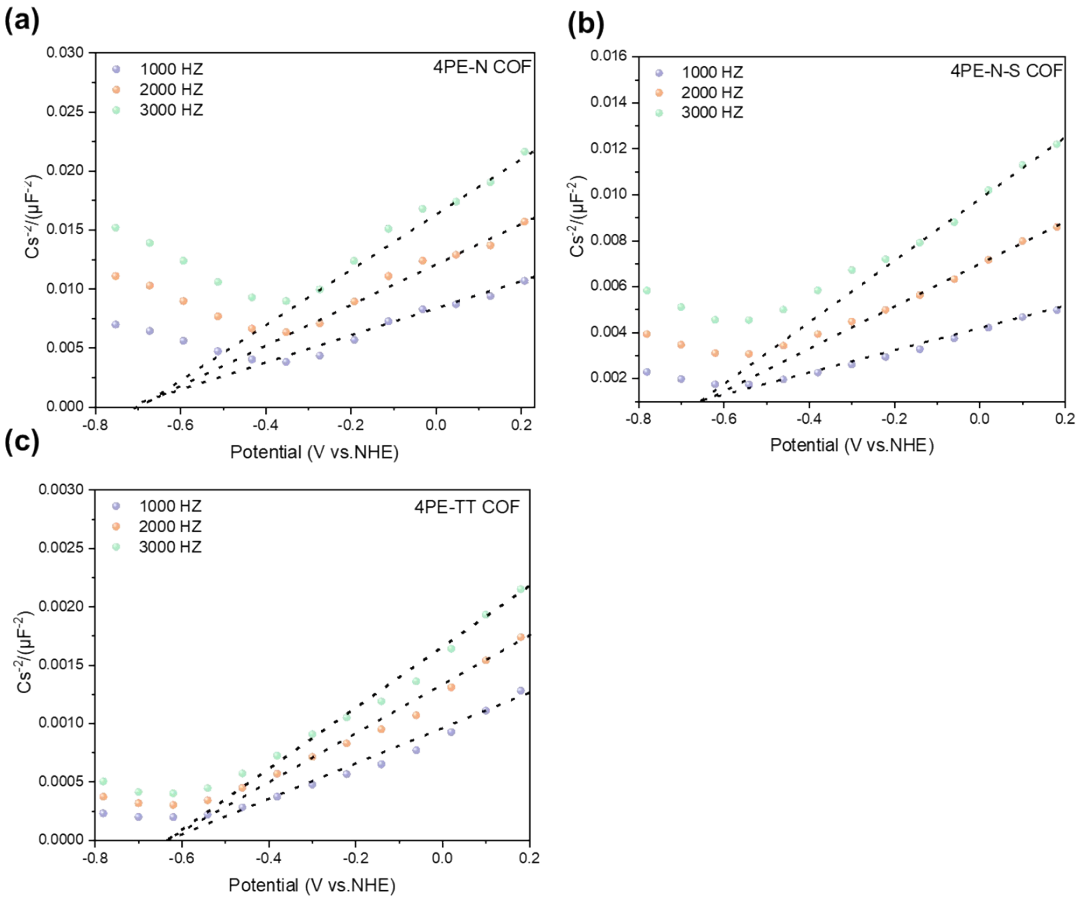

Figure S13. Mott-Schottky curves of (a) 4PE-N, (b) 4PE-N-S and (c) 4PE-TT COF at the isoelectric point (pH=5).

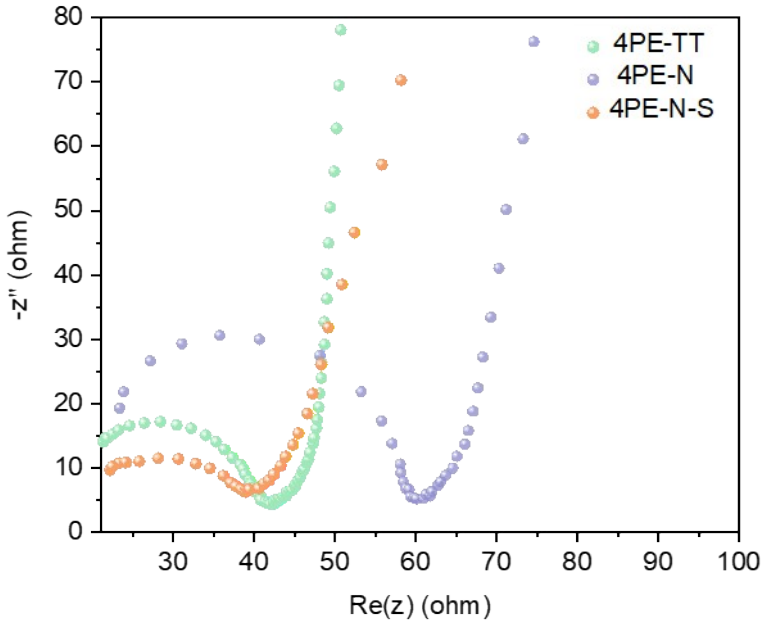

Figure S14. EIS Nyquist plots of 4PE-N, 4PE-N-S and 4PE-TT COF.

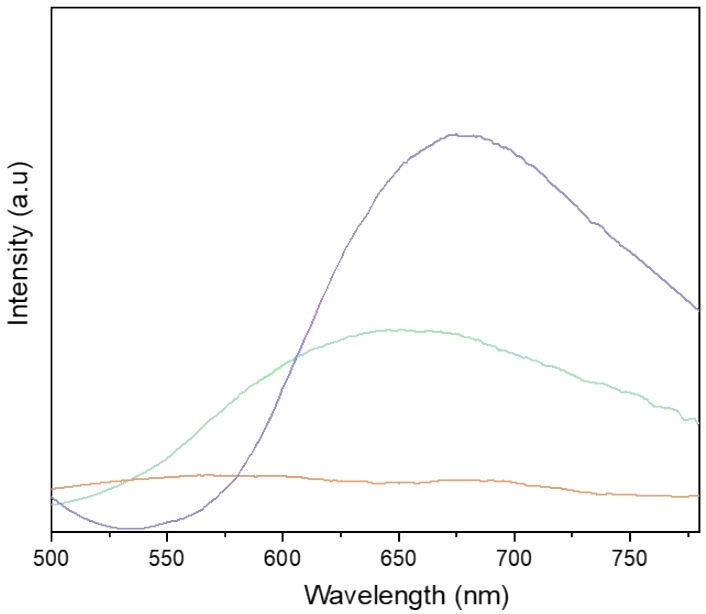

Figure S15. PL spectra (λ=350 nm) of 4PE-N, 4PE-N-S and 4PE-TT COF.

Table S5: Comparison with other representative materials in photocatalytic H_2O_2 production.

Material	H_2O_2 production rate	Irradiation conditions	Solvent	Reference
TAPD-$(Me)_2$-COF	97 μmol g^{-1} h^{-1}	λ > 420 nm	H_2O: EtOH = 9:1	4
TAPD-$(OMe)_2$-COF	91 μmol g^{-1} h^{-1}			
EBA-COF	1820 μmol g^{-1} h^{-1}	λ = 420 nm	H_2O: EtOH = 9:1	5
	1820 μmol g^{-1} h^{-1}		H_2O: Isopropanol = 9:1	
	2550 μmol g^{-1} h^{-1}		H_2O: benzyl alcohol (BA) = 9:1	
H-COF	516 μmol g^{-1} h^{-1}	λ > 400 nm	H_2O: EtOH = 9:1	6
TF-COF	1239 μmol g^{-1} h^{-1}			
TF_{50}-COF	1739 μmol g^{-1} h^{-1}			
COF-TfpBpy	1042 μmol g^{-1}	λ > 420 nm	H_2O	7

TPB-DMTP-COF	606 μmol g^{-1} h^{-1} (O_2-presaturated water)	$\lambda > 420$ nm	H_2O	[8]
	1565 μmol g^{-1} h^{-1} (continuous O_2 bubble)			
CTF-BDDBN	97 μmol g^{-1} h^{-1}	$\lambda > 420$ nm	H_2O	[9]
CTF-NS-5BT	1630 μmol g^{-1} h^{-1}	$\lambda > 420$ nm	H_2O: BA = 9:1	[10]
g-C_3N_4/PDI-BN0.2-$rGO_{0.05}$	30.8 μmol g^{-1} h^{-1}	$\lambda > 420$ nm	H_2O	[11]
CoPc-BTM-COF	2096 μmol g^{-1} h^{-1}	$\lambda > 400$ nm	H_2O: EtOH = 9:1	[12]
CoPc-DAB-COF	1851μmol g^{-1} h^{-1}	$\lambda > 400$ nm	H_2O: EtOH = 9:1	[12]
1H-COF	44.5 μmol L^{-1} h^{-1}	$\lambda > 420$ nm	10 vol% IPA	[13]
4PE-N	270 μmol g^{-1} h^{-1}	$\lambda > 420$ nm	H_2O	**This work**
	546 μmol g^{-1} h^{-1}		H_2O: EtOH = 9:1	
	436 μmol g^{-1} h^{-1}		Real seawater	
	624 μmol g^{-1} h^{-1}		Real seawater: EtOH = 9:1	
4PE-TT	421 μmol g^{-1} h^{-1}		H_2O	
	624 μmol g^{-1} h^{-1}		H_2O: EtOH = 9:1	
	795 μmol g^{-1} h^{-1}		Real seawater	

	881 μmol g^{-1} h^{-1}		Real seawater: EtOH = 9:1	
4PE-N-S	1574 μmol g^{-1} h^{-1}		H_2O	
	2237 μmol g^{-1} h^{-1}		H_2O: EtOH = 9:1	
	1940 μmol g^{-1} h^{-1}		Real seawater	
	2556 μmol g^{-1} h^{-1}		Real seawater: EtOH = 9:1	

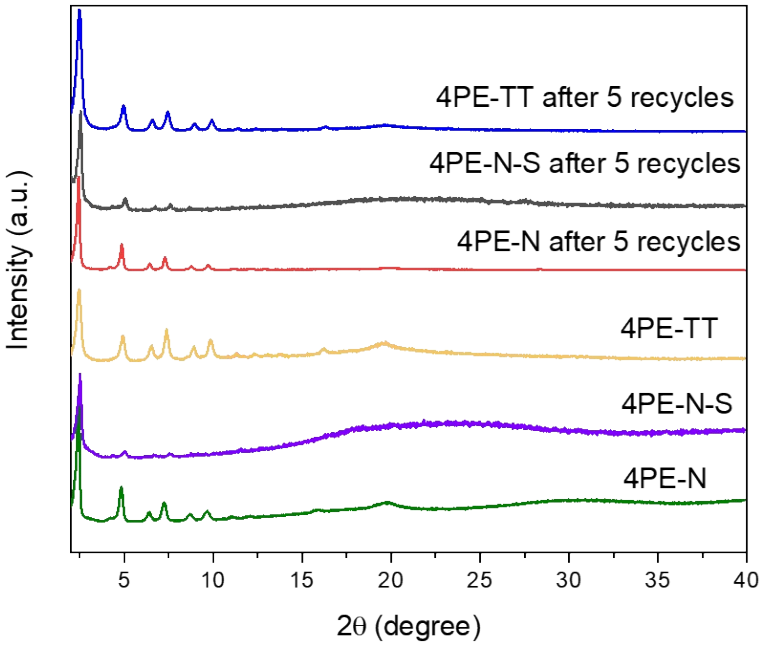

Figure S16. The pristine PXRD patterns and experimental patterns of 4PE-N, 4PE-TT and 4PE-N-S COFs after 5 recycles.

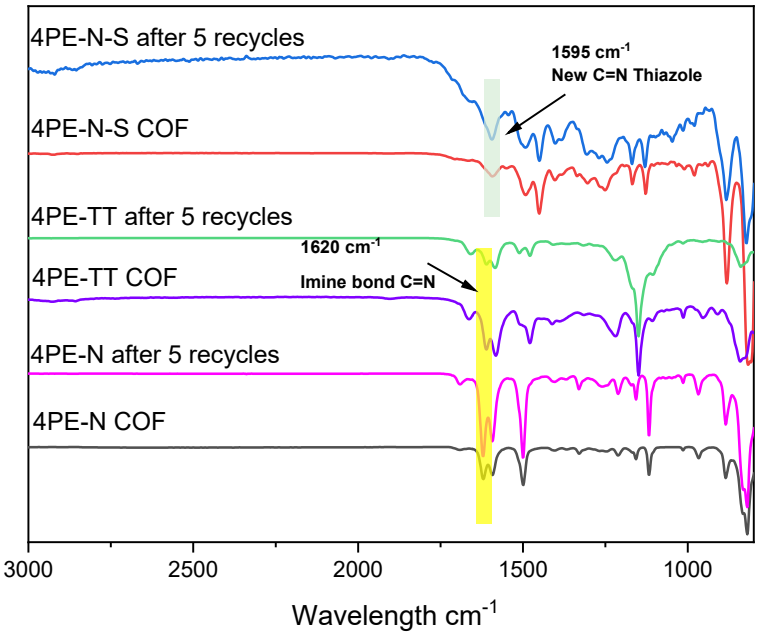

Figure S17 FT-IR spectra of the 4PE-N, 4PE-N-S and 4PE-TT COF and three spent COFs (after 5 recycles).

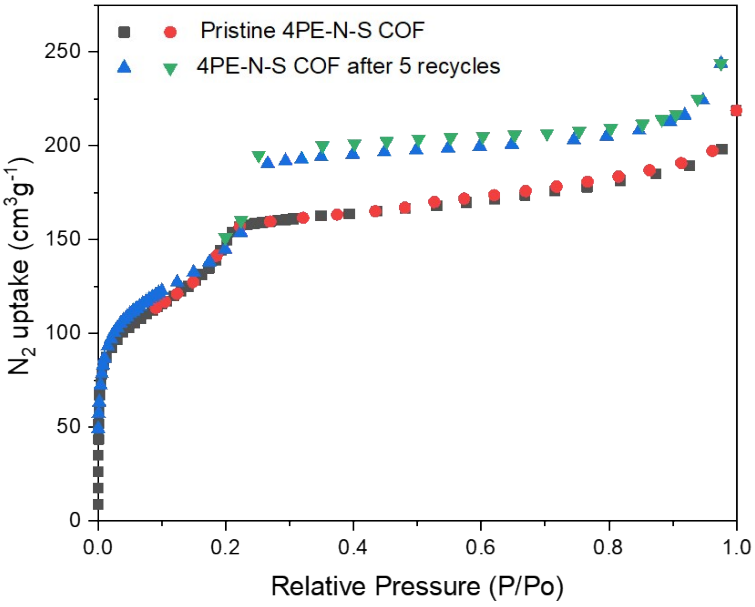

Figure S18. The N_2 adsorption/desorption isotherms for pristine 4PE-N-S COF and after 5 recycles.

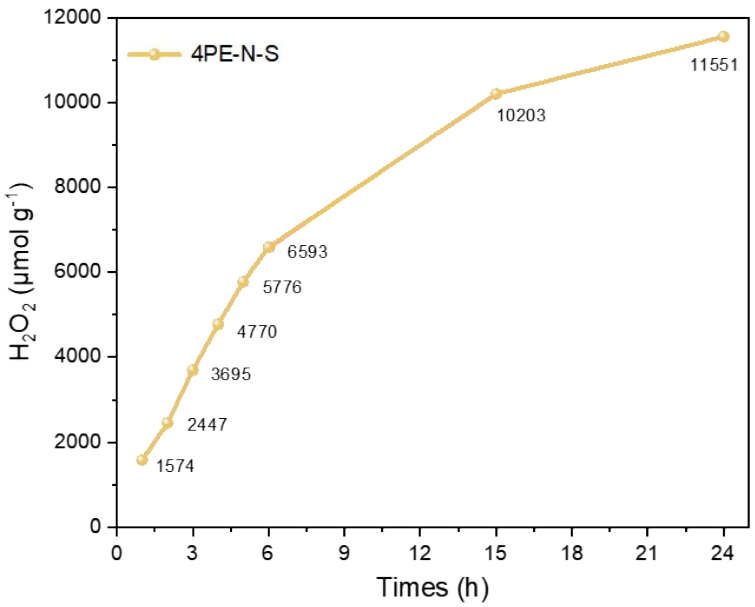

Figure S19. Time course of photogenerated H_2O_2 of 4PE-N-S COF in pure water system.

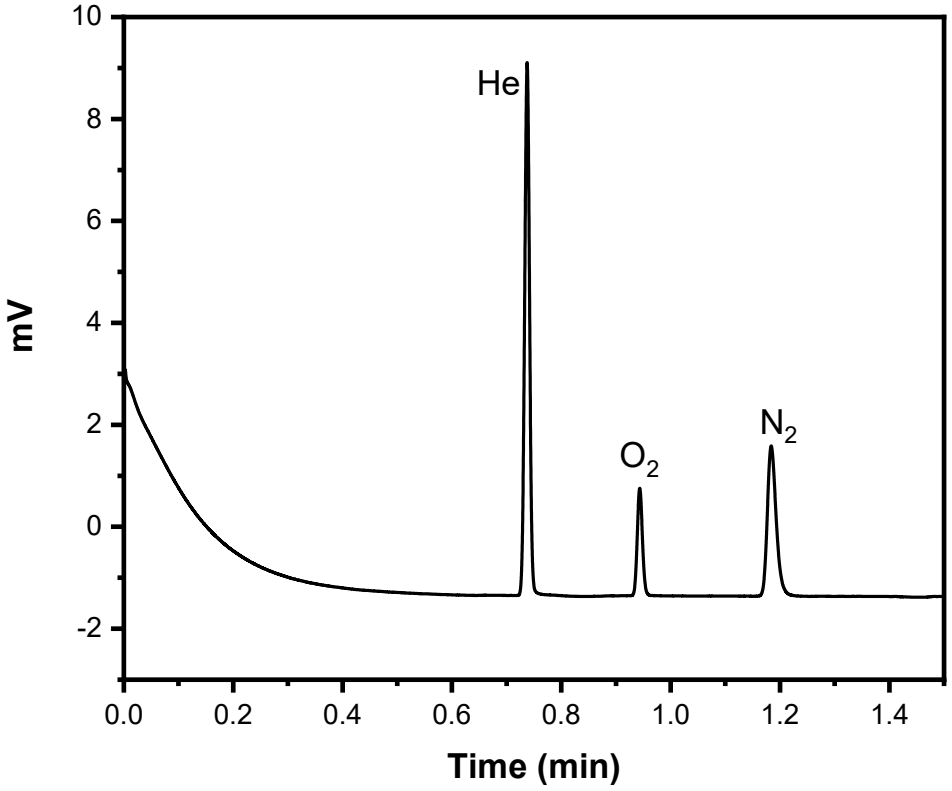

Figure S20. The production of O_2 via ORR reaction (Helium as internal standard).

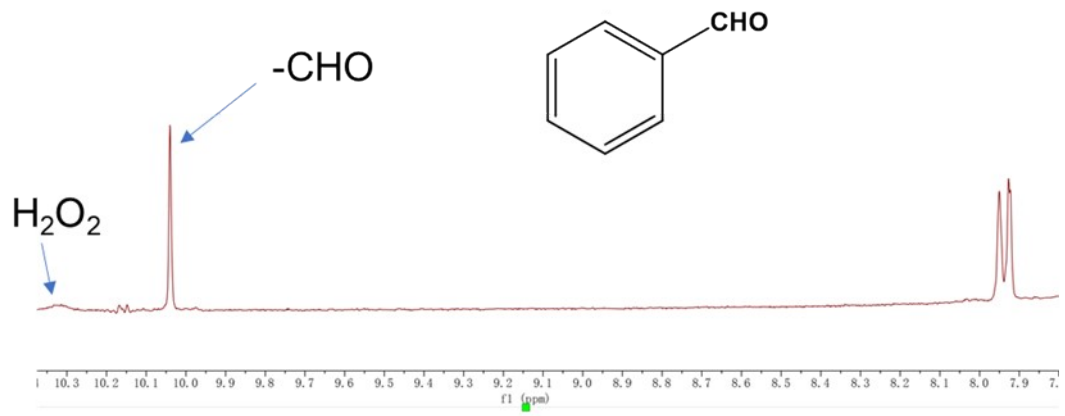

Figure S21. Formation of benzaldehyde after using BA as a sacrificial agent after 2 hours in water/BA (1:9) system.

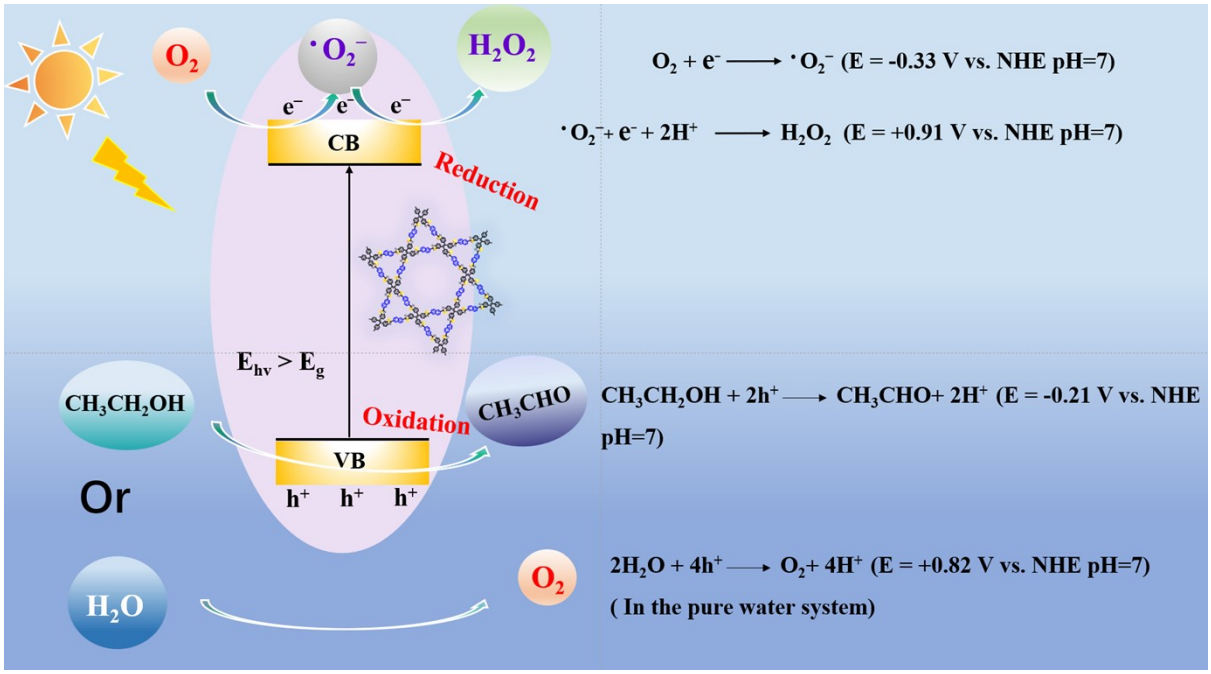

Figure S22. Proposed mechanism for the photocatalytic formation of hydrogen peroxide.

5. Photocatalytic H_2O_2 production experiments. Typically, 5 mg of the as-synthesized COF powder was dispersed in 10 mL milli-Q water in a glass vial (20 mL). The suspension was well dispersed by ultrasonication for 10 min and O_2 was bubbled into the suspension for 15 min in dark. Prior to the photocatalytic test, the suspension was stirred for 20 min in the dark to reach the adsorption-desorption equilibrium. A 300 W lamp with a 420-700 nm wavelength was irradiated on the glass vial in a dark room

(light intensity = 5.46 W m ^{2}). The reaction temperature was maintained at 25 °C with a circulating water bath. The distance between the reactor and the light source was kept fixed at 15 cm and the stirring speed was maintained at 600 rpm. After the reaction, the reaction mixture was filtrated with a 0.22 μm syringe filter to remove the photocatalysts. The concentration of H_2O_2 was determined by using an UV-vis spectrophotometer. The sample was mixed with a pre-prepared $[Ti(OH)3(H2O)3]^{+}_{(aq)}$ solution and the concentration of H_2O_2 concentration was determined by means of the UV-vis spectrometry. The UV spectrophotometry $[Ti(O_2)OH(H_2O)_3]^{+}_{(aq)}$ color method follows the reaction (Eq. S2), in which the colorless $[Ti(OH)_3(H_2O)_3]^{+}_{(aq)}$ reacts with H_2O_2 to generate a yellow peroxotitanium complex $[Ti(O_2)OH(H_2O)_3]^{+}_{(aq)}$ whose absorbance (A) can be measured at 409 nm (Eq. S2) see Figure S23 below.

$$TiOSO_{4(s)} + 5H_2O \leftrightarrow [Ti(OH)3(H2O)3] + (aq) + HSO_4^{-}(aq) \quad (\text{Eq. S1})$$

$$[Ti(OH)3(H2O)3] + (aq) + H2O2\ (aq) \leftrightarrow [Ti(O2)OH(H2O)3] + (aq) + 2H_2O \quad (\text{Eq. S2})$$

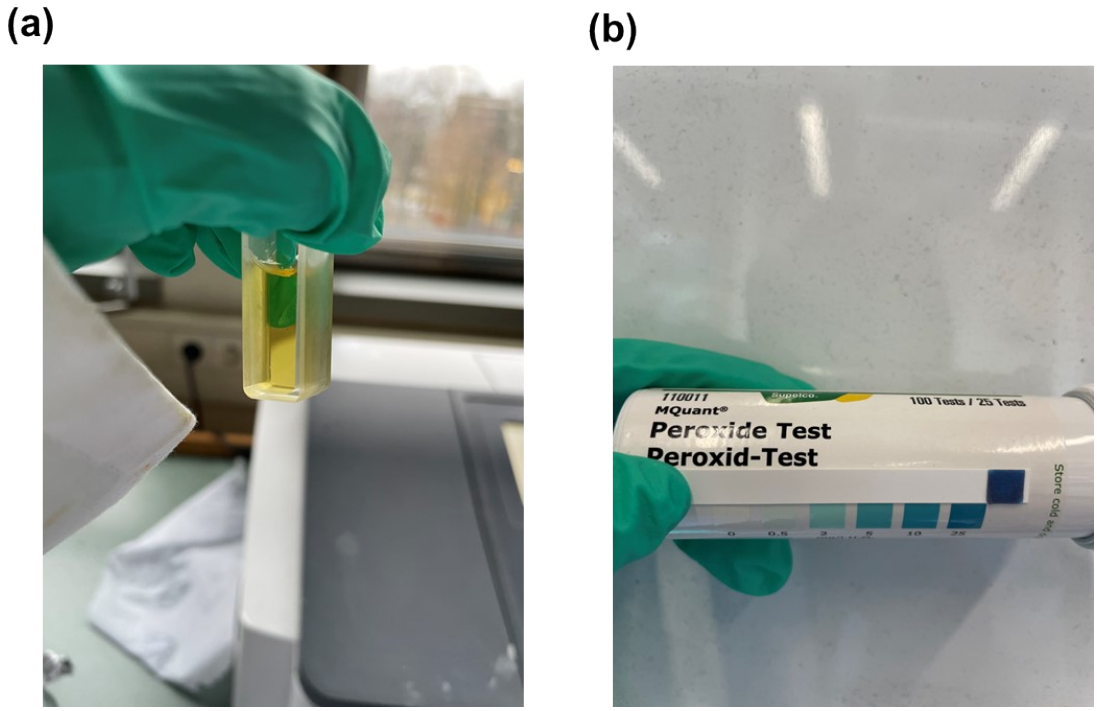

Figure S23. (a) The color of the peroxotitanium complex $[Ti(O_2)OH(H_2O)_3]^{+}_{(aq)}$, (b) peroxide test after 15 hours in pure water system.

The unknown concentration of H_2O_2 can be calculated by calibration curve. The calibration curve was established by absorption intensity (A) and known concentration of H_2O_2 solution. The linear relationship between absorption intensity and H_2O_2 concentration was established as follows:

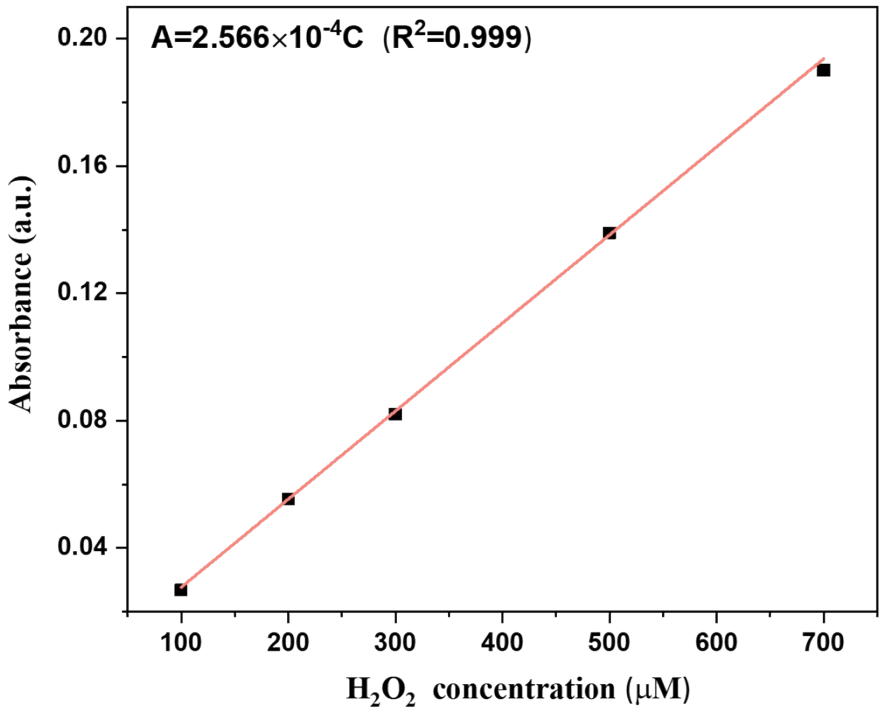

Based on the calibration curve, the H_2O_2 concentration could be determined.

Photocurrents and photoelectrochemical measurements: 5 mg of the catalysts were dispersed in a mixture containing 1 mL ethanol, and 10 μL Nafion. The mixture was sonicated for 1 hour to form a homogenous catalyst ink. 100 μL of this catalyst ink was drop-casted on a polished 1 cm × 2 cm area of an FTO glass and dried in air. These measurements were conducted on a CHI 660E electrochemical work station in a three-electrode cell system under irradiation of with 300 W Xe lamp (Perfect Light PLS-SXE 300+) with a ≥ 420 nm cutoff filter. A Pt wire and Ag/AgCl electrode were used as the working electrode and the reference electrode, respectively. A 0.1 M Na_2SO_4 solution was utilized as

the electrolyte. The Mott-Schottky measurement was performed at frequency of 1000, 2000 and 3000 Hz respectively in dark conditions. Prior, the isoelectric point was determined by measuring the zeta-potential at different pH (Zetasizer (NanoZS), Malvern). The electrochemical impedance spectroscopy (EIS) was carried out at a bias potential of +0.5 V in the dark.

Photo luminescence measurements: The luminescence excitation and emission spectra were recorded using an Edinburgh Instruments FLSP920 UV-vis-NIR spectrometer setup with a 450 W xenon lamp as the steady state excitation source. The emission signals were detected using a Hamamatsu R928P photomultiplier tube. All emission spectra in the manuscript have been corrected for detector response. Luminescence decay times were recorded using a 60 W pulsed xenon lamp, operating at a frequency of 100 Hz. Colloidal suspensions of the COFs were measured in quartz cuvettes with a path length of 10 mm.

References:

1. Anuradha, D. D. La, M. Al Kobaisi, A. Gupta and S. V. Bhosale, *Chem. Eur. J.*, 2017, **23**, 3950-3956.
2. G.-Y. Xie, L. Jiang and T.-B. Lu, *Dalton trans.*, 2013, **42**, 14092-14099.
3. A. C. Jakowetz, T. F. Hinrichsen, L. Ascherl, T. Sick, M. Calik, F. Auras, D. D. Medina, R. H. Friend, A. Rao and T. Bein, *J. Am. Chem. Soc.*, 2019, **141**, 11565-11571.
4. C. Krishnaraj, H. Sekhar Jena, L. Bourda, A. Laemont, P. Pachfule, J. Roeser, C. V. Chandran, S. Borgmans, S. M. J. Rogge, K. Leus, C. V. Stevens, J. A. Martens, V. Van Speybroeck, E. Breynaert, A. Thomas and P. Van Der Voort, *J. Am. Chem. Soc.*, 2020, **142**, 20107-20116.
5. L. Zhai, Z. Xie, C.-X. Cui, X. Yang, Q. Xu, X. Ke, M. Liu, L.-B. Qu, X. Chen and L. Mi, *Chem. Mater.*, 2022, **34**, 5232-5240.
6. H. Wang, C. Yang, F. Chen, G. Zheng and Q. Han, *Angew. Chem. Int. Ed.*, 2022, **61**, e202202328.
7. M. Kou, Y. Wang, Y. Xu, L. Ye, Y. Huang, B. Jia, H. Li, J. Ren, Y. Deng and J. Chen, *Angew. Chem. Int. Ed.*, 2022, **61**, e202200413.
8. L. Li, L. Xu, Z. Hu and J. C. Yu, *Adv. Funct. Mater.*, 2021, **31**, 2106120.
9. L. Chen, L. Wang, Y. Wan, Y. Zhang, Z. Qi, X. Wu and H. Xu, *Adv. Mater.*, 2020, **32**, 1904433.
10. X. Yu, B. Viengkeo, Q. He, X. Zhao, Q. Huang, P. Li, W. Huang and Y. Li, *Adv. Sustain. Syst.*, 2021, **5**, 2100184.
11. Y. Kofuji, Y. Isobe, Y. Shiraishi, H. Sakamoto, S. Ichikawa, S. Tanaka and T. Hirai, *ChemCatChem*, 2018, **10**, 2070-2077.
12. Q. Zhi, W. Liu, R. Jiang, X. Zhan, Y. Jin, X. Chen, X. Yang, K. Wang, W. Cao, D. Qi and J. Jiang, *J. Am. Chem. Soc.*, 2022, DOI: 10.1021/jacs.2c09482.

13. H. Hu, Y. Tao, D. Wang, C. Li, Q. Jiang, Y. Shi, J. Wang, J. Qin, S. Zhou and Y. Kong, *J. Colloid Interface Sci.*, 2023, **629**, 750-762.